

FFSM Studies of Transient Eddies in the MGS TES Temperature Data.

J.R. Barnes, *College of Oceanic and Atmospheric Sciences, Oregon State University, Corvallis, OR 97331*
(*barnes@oce.orst.edu*).

Introduction:

Planetary eddies are key components of the atmospheric general circulation and climate system of Mars. Transient eddies have been known to be prominent in winter since the Viking meteorology observations (1,2), as have thermal tides. Quasi-stationary eddies were predicted by GCM studies, and their existence has now been confirmed by MGS TES and RS data. The MGS TES atmospheric temperature data have also allowed a basic characterization of the transient eddies, subject to the relatively coarse vertical resolution of these profiles (3,4). MGS RS data have permitted determination of the properties of the transient eddies at much higher vertical resolution, but without the global coverage of the TES data (5).

The TES temperature data are highly synoptic, and must be spectrally analyzed and synoptically mapped to allow study of the planetary eddies. In these studies this has been done by making use of the Fast Fourier Synoptic Mapping (FFSM) method originally developed by Salby.

Data Analysis:

The FFSM approach possesses some unique advantages in comparison with other possible methods. It allows the production of twice-daily synoptic maps possessing the full space-time resolution of the data, and does not distort or smooth higher frequency ($\sim 1-3$ sols) signals. An intermediate product of the FFSM approach is a set of space-time spectra for all of the latitudes and levels being analyzed, which can then be used to determine the dominant eddy modes in the data. In a typical FFSM analysis of the TES data, the resulting spectra have very high statistical significance, which allows even very small-amplitude modes to be identified and characterized.

Results:

Seasonal variations in eddy activity Fig. 1 shows examples (for the first mapping year) of the seasonal variation of the transient eddy activity in the northern and southern hemisphere fall, winter, and spring seasons. The transient eddy activity in the north at low levels peaks in the autumn and again in middle to late winter. At upper levels, the activity peaks – at much larger variance values – between $L_s \sim 240-270$ following the occurrence of a large regional dust storm. Each of the three years observed by TES exhibits a somewhat different seasonal variation in the upper level transient eddy activity, which in each case is clearly tied to the occurrence of large dust storms. The third mapping year is the most different, in that the upper level eddy activity exhibits two distinct peaks in autumn and in midwinter – very much as the low-level activity does. Two large regional dust storms occurred in the third year, with the

second storm beginning in midwinter at $L_s \sim 320$.

In the south there is a pronounced peak in the eddy activity in middle and late winter, at low levels. There

is also a much weaker second peak in southern autumn ($L_s \sim 30-60$), in the second and third mapping years in which there is coverage of the autumn season. The upper-level eddy activity in the south is very weak compared to that in the north, and the low-level activity is also significantly reduced (in comparison to the periods in which the low-level activity is strong in the north).

The occurrence of the strongest transient eddy activity in middle and late winter in the south may be very significant in relation to results from analyses of MGS GRS polar Argon enrichment data (6). The lack of strong eddy activity in the fall and early winter seasons could be a primary factor in allowing very large Argon enrichments to occur in the south polar region (7).

Interannual variations in eddy activity As noted above, there is very substantial interannual variability evidenced by the TES data for the transient eddy activity in the north, whereas that in the south is much smaller.

Each of the three northern winters of the mapping mission is characterized by a different timeline of eddy activity. In the first year, the start of a large regional dust storm at $L_s \sim 226$ rapidly triggered the onset of very strong upper-level eddy activity which gradually declined after solstice. A large global dust storm began at $L_s \sim 184$ in the second northern winter, but did not rapidly trigger strong upper-level transient eddy activity. The storm did strongly suppress the low-level autumn activity, in comparison to that in the first and third years. This is very similar to the sharp reduction in eddy activity observed by the Viking Landers following the first-year winter solstice dust storm (1). Very strong upper-level eddy activity began in the second MGS year by $L_s \sim 220$ (in the midst of the global dust storm), and continued until well after solstice. In the third year, there were two large regional dust storms starting prior to $L_s \sim 220$ and at $L_s \sim 320$ (just before the Spirit landing). Each of these events immediately triggered strong upper-level eddy activity, which was at an elevated level throughout the entire period between the two storms. The low-level activity prior to the first storm event was unusually strong compared to that in the first year (and much stronger than that in the second year).

Clearly, the interannual variability in the northern winter transient eddy activity is strongly tied to that in the major dust storm activity. Each mapping year is characterized by a unique timeline of major dust storm activity and the eddy activity appears to directly reflect this. The unusually strong eddy activity in the third year autumn (prior to the regional dust storm) is an example

of interannual variability which is not directly tied to dust storm variability – unless it is related to the global storm in the second year.

Storm zones Most of the time the transient eddy activity is strongly enhanced in certain longitudinal regions, storm zones, as first predicted by GCM studies (8). Several examples of these are shown in Figure 2. In the north the storm zones tend to basically coincide with the lowland regions of Acidalia, Utopia, and Arcadia, though other regions also show enhanced eddy activity at times. The northern storm zones extend to very high levels when the upper-level eddy activity is strong, with the maximum activity occurring in the ~300-360 E and ~120-180 E regions. The southern winter eddy activity is even more strongly regionalized at low-levels than that in the north, with the strongest activity being present in the ~200-300 E region. This is in the vicinity of the southern extension of Tharsis extending east to the Argyre basin. At upper levels, however, the southern hemisphere eddy activity is relatively uniform in longitude. The location of the southern storm zone may have an important influence on the location of the south polar residual polar cap and the Cryptic Region (9).

Recent work (10) has confirmed that the so-called “flushing” dust storms which are very prominent in MOC imagery of the northern hemisphere are indeed generated by strong low-level transient eddies (weather systems) in the lowland regions. Since the low-level eddy activity is at its strongest in the autumn (except in the second MGS year) and middle to late winter seasons, this is when these local dust storms occur. The large regional dust storm in the third year at $L_s \sim 320$ began as a flushing storm triggered by strong transient eddy activity in the Utopia region.

Eddy modes The transient eddy activity is characterized by certain combinations of zonal wavenumber and period - modes. The periods of these modes range from less than 2 sols to as long as 30 sols, while the wavenumber values are 1-4. The lower wavenumber modes tend to have longer periods. However, the storm zones are characterized by multiple modes having the same period, while a group of modes at different wavenumbers with periods varying commensurately is associated with a coherently propagating wave group – likely including frontal structures.

Overall, the wavenumbers and periods of the eddy modes determined by FFSM analyses of TES data are quite similar to those determined from the Viking meteorology data (1,2). Typically present are wavenumber 1 modes with periods of ~ 6-10 sols, wavenumber 2 modes with periods of ~ 3-5 sols, and wavenumber 3 modes with periods of ~ 2-3 sols. The major mode not evident in the Viking data is at wavenumber 1 and periods of ~ 15-30 sols; this mode is prominent in the northern hemisphere under dusty conditions (and is largely responsible for the very strong eddy activity at upper levels following major dust storm events).

The vertical structures of the wavenumber 1 modes can be very deep, while those of the wavenumber 3 and 4 modes tend to be quite shallow. The wavenumber 2 modes can have significant amplitudes at both lower and upper levels, as can be seen in Fig. 3.

Synoptic structure The end product of FFSM analysis is a set of synoptic maps, two per sol (though more can be generated for animations and other applications). Several examples of these maps are shown in Fig. 4. The maps show a generally complex and rapidly changing transient eddy structure – relatively strong eddies are often seen to form or decay on time scales of ~ 1 sol. The flow typically tends to be dominated by relatively large-amplitude eddies over some interval (typically ~ 3-10 sols), and then the eddies become much weaker for some period. At times the eddies are very globally coherent, while at other times only a single pair of relatively large amplitude warm and cold disturbances are present. A very interesting case of this, which is most common in the southern hemisphere, is a “backwards” system with a leading (eastward) cold sector and a trailing warm sector. Substantial meridional movement of the eddies can be seen at times in some regions – the Acidalia and Chryse regions frequently show such movement (in particular, the equatorward penetration of cold disturbances which is associated, in at least some cases, with flushing dust storms).

A basic aspect of the eddy structures is that temperatures very frequently fall below the CO₂ frost point in the cold sectors of the eddies. This behavior is very pronounced during periods following major dust storm events. In the north, temperatures can fall more than 20 K below the frost point (at low levels) and temperatures of ~ 4-10 K below the frost point are common (at both low and intermediate levels). The coldest temperatures typically are found at places and times where the cold sectors of the transient and quasi-stationary eddies (as well as the thermal tides) coincide and reinforce each other.

Summary:

The MGS TES atmospheric temperature data have allowed a basic characterization of the transient planetary eddies which are prominent in both hemispheres in winter. The FFSM analysis approach has been utilized to enable detailed studies of these eddies. The eddies exhibit very large seasonal variations in both hemispheres, and substantial interannual variability in the north. The latter is closely related to major dust storm activity. The northern winter eddy activity is significantly stronger than that in the south, especially at upper levels. Typically, the transient eddy activity varies considerably in longitude (at the latitudes where it is strongest), such that storm zones exist. In the north, the storm zones can extend to high altitudes. A wide range of eddy modes are present, and these are very similar in period to those found in the Viking meteorology data. The synoptic eddy structures can be quite complex and rapidly changing. The transient eddies play a major role in producing extremely cold polar temperatures, which can be as much as 10-25 K below the CO₂ frost point.

References:

- (1) Barnes, J.R., 1980, *J. Atmos. Sci.*, **37**, 2002-2015.
- (2) Barnes, J.R., 1981, *J. Atmos. Sci.*, **38**, 225-234.
- (3) Barnes, J.R., 2003, In *Sixth International Conference on Mars*, Abstract #3127, Lunar and Planetary Institute, Houston (CD-ROM).
- (4) Banfield, D.B., B.J. Conrath, P.J. Gierasch, R.J. Wilson,

and M.D. Smith, 2004, *Icarus*, **170**, 365-403.
 (5) Hinson, D.P., 2005, *J. Geophys. Res.*, in review.
 (6) Sprague, A.L., W.V. Boynton, K.E. Kerry, D.M. Janes, D.M. Hunten, K.J. Kim, R.C. Reedy, and A.E. Metzger, 2004, *Science*, **306**, 1364-1367.
 (7) Barnes, J.R., 2005, In *Lunar and Planetary Science XXXVI*, Abstract #1267, Lunar and Planetary Institute, Houston (CD-ROM).
 (8) Hollingsworth, J.L., R.M. Haberle, J.R. Barnes, A.F.C. Bridger, J.B. Pollack, H. Lee, and J. Schaefer, 1996, *Nature*, **380**, 413-416.
 (9) Colaprete, A., J.R. Barnes, R.M. Haberle, J.L. Hollingsworth, H.H. Kieffer, and T.N. Titus, 2005, *Nature*, **435**, 184-188, doi:10.1038.
 (10) Wang, H., R.W. Zurek, and M.I. Richardson, 2005, *J. Geophys. Res.*, **110**, E07005, doi:10.1029/2005JE002423.
 Fig. 1a: Transient eddy variance versus seasonal date in the first MGS mapping southern winter at 45, 50, and 55 S.

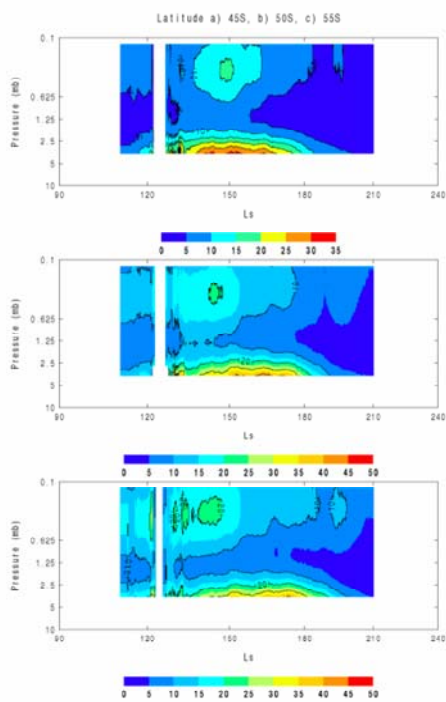


Fig. 1b: Transient eddy variance versus seasonal date in the first MGS mapping northern winter at 50, 55, and 60 N.

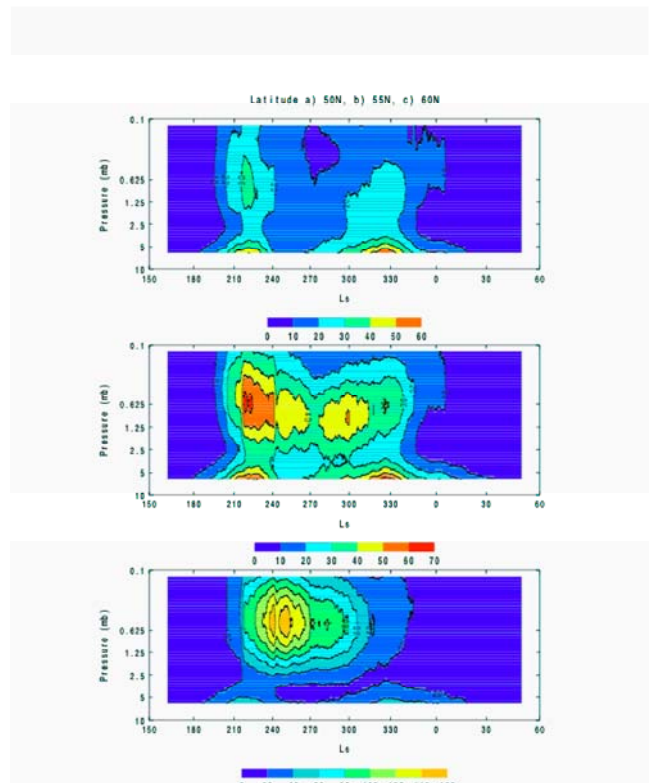


Fig. 2a: Northern storm zones (variance) at a lower level for $L_s \sim 237-270$ in the first mapping year.

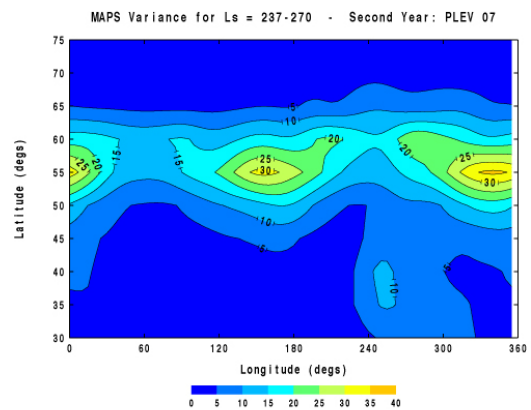


Fig. 2b: Northern storm zones (variance) at an upper level for $L_s \sim 237-270$ in the first mapping year.

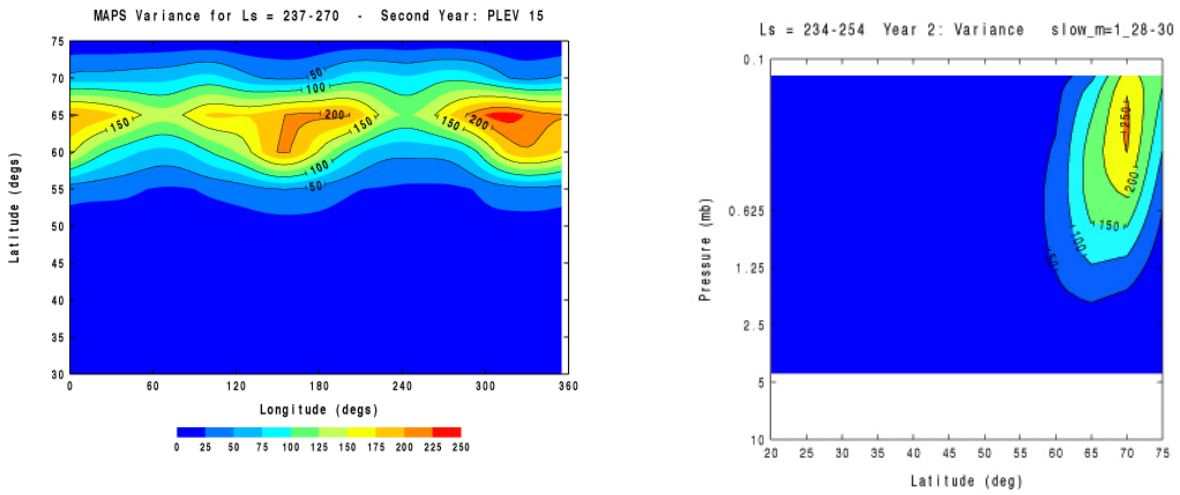


Fig. 2c: Southern storm zone (variance) at a lower level for $L_s \sim 136-155$ in the first mapping year.

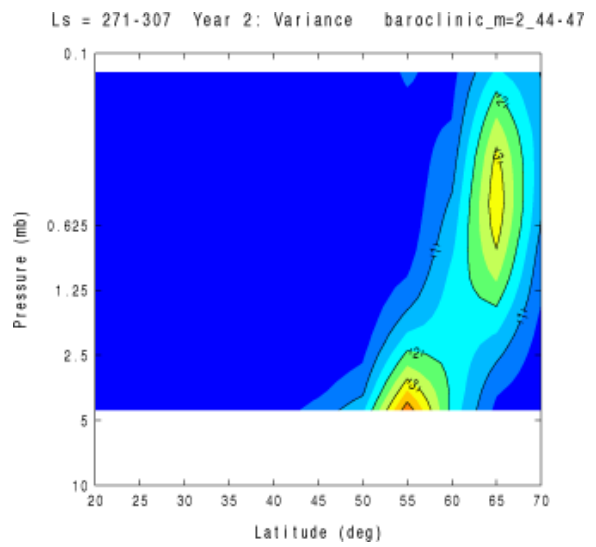
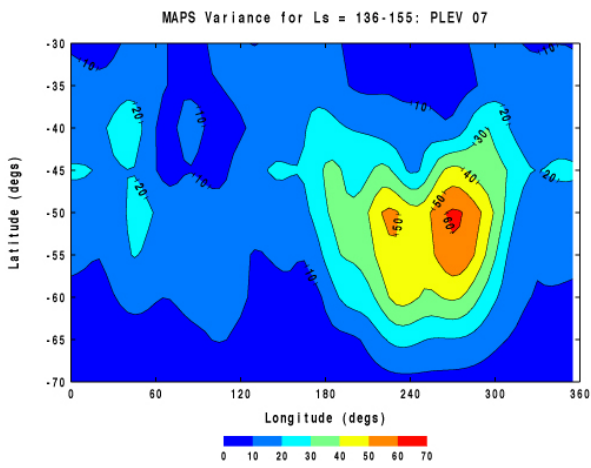


Fig. 3: A wavenumber 1 eddy mode (top), a wavenumber 2 mode (middle), and a wavenumber 4 mode (bottom).

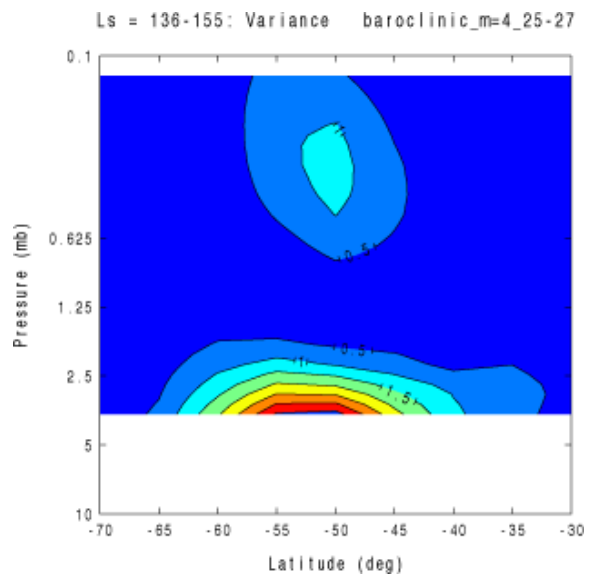


Fig. 4: Synoptic transient eddy maps: a dominant wave 2 pattern in northern autumn (top), a very large-amplitude wave

1 pattern in northern winter (middle), and a wavenumber 3 pattern in southern winter (bottom).

